Available online at www.sciencedirect.com

ScienceDirect

Journal of the Franklin Institute 352 (2015) 5779–5795

Journal of The Franklin Institute

www.elsevier.com/locate/jfranklin

Coordinated formation control design with obstacle avoidance in three-dimensional space

Kai Chang[a], Yuanqing Xia[b,*], Kaoli Huang[a]

[a]School of Automation, Mechanical Engineering College, Shijiazhuang 050003, China
[b]School of Automation, Beijing Institute of Technology, Beijing 100081, China

Received 2 September 2014; received in revised form 18 May 2015; accepted 5 October 2015
Available online 22 October 2015

Abstract

This paper considers a problem of coordination formation control for multiple unmanned vehicles based on the behavioral control and virtual structures in three-dimensional space. The repulsive forces effect among unmanned vehicles to avoid collision with others and move them to the balance points on the spherical surface whose center is the virtual leader. The unmanned vehicles do not have specific identities or roles within the formation. The proposed method does not require specific orders or positions of the unmanned vehicles. The formation can transform automatically when unmanned vehicles enter or exit the formation. This paper also proposes a technique for avoiding obstacles based on the behavioral structure. In this technique, when an unmanned vehicle gets close to an obstacle, while moving toward its target, two kinds of potential fields with rotational vectors are applied to lead the unmanned vehicle to avoid the obstacle. Simulations are also given to verify the effectiveness of theoretical results.

1. Introduction

The formation control of unmanned vehicles such as unmanned aerial vehicles (UAVs), mobile robots and autonomous underwater vehicles (AUVs) has been the subject of extensive research in recent years. Among them, unmanned vehicles group can improve task allocation, performance, the time duration required, the system effectiveness and the safety to achieve the desired outcome [1–3].

*Corresponding author. Tel.:+86 10 68914350.
E-mail addresses: kerkaichance@gmail.com (K. Chang), xia_yuanqing@bit.edu.cn (Y. Xia), huangkaoli@163.com (K. Huang).

http://dx.doi.org/10.1016/j.jfranklin.2015.10.002
0016-0032/

Different architectures, strategies and methods have been proposed to control and coordinate the unmanned vehicles formation. The main methods include behavior-based, virtual structure, leader–follower. Every method has its own advantages and disadvantages. In the behavioral approach, the control action for each vehicle is derived by a weighted average of each desired behavior [4]. However, it is lack of modeling for the subsystems or unmanned vehicle surroundings. In the leader–follower method, one of the unmanned vehicles is designated as the leader, with the rest unmanned vehicles as followers. In this method, there is no explicit feedback from the followers to the leader. Paper [8] proposes a distributed control scheme with distributed estimators. It is supposed that the followers only need relative positions in a noisy environment. In [9], the leader position and predetermined formation are achieved without need for leaders velocity and dynamic. The virtual leader structure consists of replacing a formation leader, in the leader–follower structure, by a virtual one. All the UAVs in the formation receive the mission trajectory. This trajectory is the virtual leader itself. One of the main drawbacks of this structure is that the possibility of collision between UAVs increases, since there is no feedback to the formation. In the virtual structure approach, the entire formation is treated as a single rigid body. The control law for a single vehicle is derived by defining the dynamics of the virtual structure and translates the motion of the virtual structure into the desired motion for each vehicle. In [14], a combination of the virtual structure and path following approaches is used to derive the formation architecture. It is extended to consider the formation controller by taking the physical dimensions and dynamics of the robots into account. The disadvantage of the current virtual structure implementation is the centralization. Failure of a single vehicle may cause the whole system to fail.

Furthermore, the model uses a combination of the Lyapunov technique and graph theory embedded in the virtual structure to recover the formation from position sensor measurement errors and temporary delays or failures in the communication [15]. The paper [6] presents a region-based shape controller for a swarm of robots. This control method maintains each robot in the group with a minimum distance from each other. The swarm of robots moves as a group and can be formed as various shapes without entire community. In [7,10], the formation control of a team mobile robots based on the virtual and behavioral structures is considered. The repulsive force method has been employed to keep formation with regular polygon. In this paper, we further investigate the virtual and behavioral structure formation control problem for unmanned vehicles in three-dimensional space. The unmanned vehicles reach the balance points on the spherical surface that resultant force from center formation and their neighbors is zero. Then, the formation is achieved. By giving a virtual leader as the center point of the formation, unmanned vehicles can adjust the position to keep the formation when the virtual leader is moving. Comparing with [5], the main advantage of proposed method is that the formation can transform into the new structure when some unmanned vehicles enter or exit the formation during the maneuver.

The existence of local minima in multiple unmanned vehicles system with potential field avoidance obstacle is a common problem. The UAV may get stuck in a local optima that the highest potential is at the current position of the UAV, and that position is not the end destination [11–13]. In [16], the potential field method is extended by combining the canonical vector field formulation with the dual Lyapunov analysis of decentralized potential fields. A density function is provided for a single robot driven by a navigation function in a static obstacle workspace. In these approaches, the formation is rigid as the geometric relationship among the unmanned vehicles in the system which must be rigidly maintained during the movement. Therefore, it is generally not possible for formation rebuilding in the case of the change in the number of unmanned vehicles and obstacle avoidance is another problem. In [17], a novel potential field whose vectors are around the obstacle is used to avoid collision. The advantage is avoiding slowing down the unmanned aircraft during the process. However, this method is lack of path optimization. In paper [18], it provides an optimal path for obstacle avoidance with calculating a path based on geometric strategies and visual identification of the environment. The

disadvantage is that unmanned vehicles in formation are only commanded to stay close together and avoid collision among themselves. In this paper, we propose a novel method for formation movement and obstacle avoidance. The unmanned vehicles do not have specific identities and roles in formation. The distance between unmanned vehicles can be adjusted immediately and the formation reconfigures automatically when unmanned vehicles enter or exit the formation.

An important problem in swarming of multiple unmanned vehicles systems is to maintain the stability and cohesion when unmanned vehicles avoid obstacle. In this paper, the potential fields with rotational vectors are divided into two kinds of potential fields, the potential fields parallel to x–y plane and the potential fields parallel to y–z plane. Each kind of potential fields has two directions of rotational vectors. The rotational vectors are adjusted to the direction of an unmanned vehicle to lead it toward its target without locating in minimum position. We use this technique to compare the two potential fields with rotational vector, choose the in smoother and shorter trajectory for each unmanned vehicle and reconfigurate the formation for the swarm formation.

The rest of paper is organized as follows: In Section 2, dynamics of unmanned vehicles model is defined. The proposed method of formation based on virtual leader is presented in Section 3. Section 4 improves the method for obstacle avoidance and extends the method into unmanned vehicle formation. Section 5 gives the simulation results. Section 6 gathers our conclusions and ideas for future work.

2. Unmanned vehicle model definition

First, we consider a multiple unmanned vehicles system that every unmanned vehicle moves without motion constraints. The control force is assumed to be completely decoupled. The nth unmanned vehicle's dynamical equations can be described as follows:

$$\begin{aligned} M\ddot{x}_n + D\dot{x}_n &= f_{x_n} - k\dot{x}_n \\ M\ddot{y}_n + D\dot{y}_n &= f_{y_n} - k\dot{y}_n \\ M\ddot{z}_n + D\dot{z}_n &= f_{z_n} - k\dot{z}_n \end{aligned} \tag{1}$$

where M is unmanned vehicle's mass, (x_n, y_n, z_n) is Cartesian coordinates of position of unmanned vehicle, $(\dot{x}_n, \dot{y}_n, \dot{z}_n)$ is Cartesian coordinates of velocity of unmanned vehicle, D is the damping coefficient that shows the drag force effect, $(f_{x_n}, f_{y_n}, f_{z_n})$ is the control force at coordinate axis direction in three-dimensional space. k is the response coefficient that considered to the transient response of unmanned vehicle. It can be adjusted. Increasing the value of k will decrease the overshoot of the unmanned vehicle system but decrease the speed of the unmanned vehicle.

3. Formation

In this section, a method for unmanned vehicles formation based on virtual leader is presented. The control force $(f_{x_n}, f_{y_n}, f_{z_n})$ guides the nth unmanned vehicle toward the spherical surface whose center is (x_c, y_c, z_c) and radius is α. Under the control strategy the unmanned vehicles will keep a safe distance from other unmanned vehicles and be evenly distributed on the spherical surface.

3.1. The nth unmanned vehicle moving control

Lemma 3.1 provides a trajectory that unmanned vehicle moves to a spherical surface whose center is (x_c, y_c, z_c) and radius is α. It is stable when the unmanned vehicle reach the spherical surface. In other words velocity of unmanned vehicle will be zero.

Lemma 3.1. *The desired trajectory of unmanned vehicle satisfies*

$$\begin{aligned}\dot{x} &= -(x-x_c)\left((x-x_c)^2+(y-y_c)^2+(z-z_c)^2-\alpha^2\right)\\ \dot{y} &= -(y-y_c)\left((x-x_c)^2+(y-y_c)^2+(z-z_c)^2-\alpha^2\right)\\ \dot{z} &= -(z-z_c)\left((x-x_c)^2+(y-y_c)^2+(z-z_c)^2-\alpha^2\right)\end{aligned} \tag{2}$$

where $(x,y,z)\neq(x_c,y_c,z_c)$.

By inserting $r^2=(x-x_c)^2+(y-y_c)^2+(z-z_c)^2$, $\varphi=\arctan\left((y-y_c)/x-x_c\right)$ and $\theta=\arctan\left((z-z_c)\Big/\left(\sqrt{(y-y_c)^2+(x-x_c)^2}\right)\right)$ into Eq. (1). φ and θ are shown in Fig. 1. The equations can be achieved as follows:

$$\dot{r}=-r\left(r^2-\alpha^2\right),\quad \dot{\theta}=0,\quad \dot{\varphi}=0 \tag{3}$$

To prove the stability of unmanned vehicle arriving at the spherical surface, it is obvious that $\dot{\theta}$ and $\dot{\varphi}$ converge to zero when $r=\alpha$, we define the error $e=r-\alpha$ and choose the following Lyapunov function candidate:

$$V(e)=e^2 \tag{4}$$

The derivative of the Lyapunov function (4) is given by

$$\dot{V}(e)=2e\dot{r} \tag{5}$$

Substituting Eq. (3) into Eq. (5), we have

$$\dot{V}(e)=-2e^2r(r+\alpha) \tag{6}$$

Because $(x,y,z)\neq(x_c,y_c,z_c)$, it can be deuced that $r>0$. It is obvious that $\dot{V}(e)\leq 0$. Since $V(e)=0$ only if $r=\alpha$, it follows that velocity is non-increasing, $\dot{\theta}=0$, $\dot{\varphi}=0$ and $V(e)$ is bounded. In other words, unmanned vehicle's trajectory converges to the spherical surface.

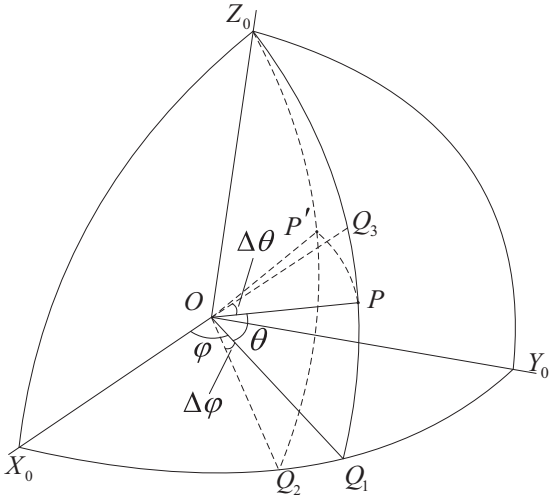

Fig. 1. Direction of the unmanned vehicle movement.

Unmanned vehicle will have no rotational motion when arrives at the spherical surface. By extending Lemma 3.1, a method for leading an unmanned vehicle toward the spherical surface can be obtained. The control force $(f_{x_n}, f_{y_n}, f_{z_n})$ in Eq. (1) is designed as follows:

$$\begin{aligned} f_{x_n} &= -k_s(x_n - x_c)\left((x_n - x_c)^2 + (y_n - y_c)^2 + (z_n - z_c)^2 - \alpha^2\right) \\ f_{y_n} &= -k_s(y_n - y_c)\left((x_n - x_c)^2 + (y_n - y_c)^2 + (z_n - z_c)^2 - \alpha^2\right) \\ f_{z_n} &= -k_s(z_n - z_c)\left((x_n - x_c)^2 + (y_n - y_c)^2 + (z_n - z_c)^2 - \alpha^2\right) \end{aligned} \tag{7}$$

where k_s is the gain coefficient. The next subsection provides the multiple unmanned vehicles control strategy for building up a formation that unmanned vehicles are evenly distributed on the spherical surface. This strategy can be used in problem of controlling pursuer convoy in three-dimensional space.

3.2. Unmanned vehicle formation

In order to arrange the unmanned vehicles evenly distributed on the spherical surface, we define a virtual leader as the center at (x_c, y_c, z_c) and all unmanned vehicles have negatively or positively charged. The repulsive forces have effect on the unmanned vehicles which have identical electric charge. The control force that defined in Eq. (7) keeps the unmanned vehicles on the spherical surface whose radius is α and center is (x_c, y_c, z_c). The unmanned vehicle reaches the balance point when the resultant of repulsive forces tangent to the spherical surface acting on an unmanned vehicle is zero. It means that the distances between unmanned vehicles are equal. Then, the goal is achieved. To attain the above conditions, the control force must be larger than the resultant of the repulsive forces in the direction of the spherical surface radius when the unmanned vehicle reaches the sphere. The repulsive force between two unmanned vehicles is defined as follows:

$$F_{ni} = k_r \frac{q_n q_i}{r_{ni}^2} \tag{8}$$

where q_n is electric quantity of the nth unmanned vehicle, q_i is electric quantity of the ith unmanned vehicle, k_r is the repulse constant coefficient, r_{ni} is the distance between the ith and the nth unmanned vehicle. The amount of unmanned vehicle is N. Hence, the resultant of the repulsive forces from the other unmanned vehicles on the nth unmanned vehicle is given as follows:

$$F_n = k_r q_n \sum_{i=1, i\neq n}^{N} \frac{q_i}{r_{ni}^2} \tag{9}$$

By decomposing the resultant force in three directions, component forces are in the x-axis direction, y-axis direction and the z-axis direction, respectively. It is shown as follows:

$$F_{xn} = k_r q_n \sum_{i=1, i\neq n}^{N} \frac{q_n q_i}{r_{ni}^2} \cos\theta_{ni} \cos\varphi_{ni}$$

$$F_{yn} = k_r q_n \sum_{i=1, i\neq n}^{N} \frac{q_n q_i}{r_{ni}^2} \cos\theta_{ni} \sin\varphi_{ni}$$

$$F_{zn} = k_r q_n \sum_{i=1, i\neq n}^{N} \frac{q_n q_i}{r_{ni}^2} \sin\theta_{ni} \tag{10}$$

where

$$\sin\theta_{ni} = \frac{z_n - z_i}{|r_{ni}|}$$
$$\cos\theta_{ni} = \frac{\sqrt{(x_n - x_i)^2 + (y_n - y_i)^2}}{|r_{ni}|}$$
$$\cos\varphi_{ni} = \frac{x_n - x_i}{\sqrt{(x_n - x_i)^2 + (y_n - y_i)^2}}$$
$$\sin\varphi_{ni} = \frac{y_n - y_i}{\sqrt{(x_n - x_i)^2 + (y_n - y_i)^2}}$$
$$r_{ni} = \sqrt{(x_n - x_i)^2 + (y_n - y_i)^2 + (z_n - z_i)^2}$$

Therefore, by considering the nth unmanned vehicle's dynamical equation (1), the nth unmanned vehicle's dynamical equations based on the virtual structure can be rewritten as

$$\begin{aligned} M\ddot{x}_n + D\dot{x}_n &= f_{x_n}(vs) - k\dot{x}_n \\ M\ddot{y}_n + D\dot{y}_n &= f_{y_n}(vs) - k\dot{y}_n \\ M\ddot{z}_n + D\dot{z}_n &= f_{z_n}(vs) - k\dot{z}_n \end{aligned} \tag{11}$$

where

$$f_{x_n}(vs) = F_{xn} - f_{x_n}$$
$$f_{y_n}(vs) = F_{yn} - f_{y_n}$$
$$f_{z_n}(vs) = F_{zn} - f_{z_n}$$

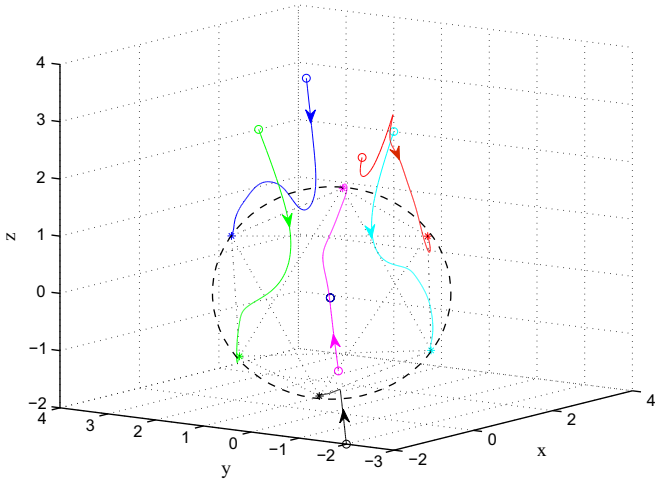

Fig. 2. Regular bipyramid formation in Example 1.

Given the above discussion, the repulsive force is proportion to $1/r_{ni}$ and keeps unmanned vehicles from the collisions. The control force ($fx_n(vs)$, $fx_n(vs)$, $fx_n(vs)$) in Eq. (11) leads the unmanned vehicles toward the balance points on the spherical surface. The following example illustrates the given formation strategy.

Example 1. Consider six unmanned vehicles whose initial positions are (2, 1, 2), (−1, −1, −1), (3, 4, 2), (4, 2, 2), (3, 3, 3) and (−2, −2, −2). The center position is (0,0,0). The control gains for unmanned vehicles are selected as $k_s=1$, $q_i=10$, $k_r=0.2$, $\alpha=2$, $k=9$. By using dynamical equations that given in Eqs. (10) and (11), the octahedron formation of the six unmanned vehicles is shown in Fig. 2. By using the proposed method, the unmanned vehicles can build up a new formation without presetting every unmanned vehicle's accurate position. Unmanned vehicles can find the balance points automatically. It is not necessary to distinguish every unmanned vehicle. The formation can transform into new structure when the number of unmanned vehicles changes. Such as the four unmanned vehicles formation shapes tetrahedroid and five unmanned vehicles shapes triangular dipyramid.

3.3. Virtual leader control

Due to the previous section, the unmanned vehicles build up the formation on the spherical surface whose center is (x_c, y_c, z_c) and radius is α. For swarm formation control, a virtual leader is considered as the center in the formation. The unmanned vehicles keep tracking the virtual leader's trajectory and adjust the positions in the formation. The control force ($fx_n(vs), fy_n(vs), fz_n(vs)$) is obtained as follows:

$$\begin{aligned} f_{x_n}(vs) &= F_{xn} - ks\Big((x_n - x_v)\Big((x_n - x_v)^2 + (y_n - y_v)^2 + (z_n - z_v)^2\Big)\Big) \\ f_{y_n}(vs) &= F_{yn} - ks\Big((y_n - y_v)\Big((x_n - x_v)^2 + (y_n - y_v)^2 + (z_n - z_v)^2\Big)\Big) \\ f_{z_n}(vs) &= F_{zn} - ks\Big((z_n - z_v)\Big((x_n - x_v)^2 + (y_n - y_v)^2 + (z_n - z_v)^2\Big)\Big) \end{aligned} \tag{12}$$

where (x_v, y_v, z_v) is the coordinate of virtual leader. The dynamical equations of the virtual leader can be written as

$$\begin{aligned} M\ddot{x}_v + D\dot{x}_v &= f_{x_v} - k\dot{x}_v \\ M\ddot{y}_v + D\dot{y}_v &= f_{y_v} - k\dot{y}_v \\ M\ddot{z}_v + D\dot{z}_v &= f_{z_v} - k\dot{z}_v \end{aligned} \tag{13}$$

where $(f_{x_v}, f_{y_v}, f_{z_v})$ is the virtual control force that define the virtual leader's trajectory. The main advantage of the proposed method is that it is not necessary to arrange the position of every unmanned vehicle. Moreover, the distance between unmanned vehicles can be adjusted automatically that order to avoid collisions in formation. The formation allows unmanned vehicles to enter or exit the formation during the maneuver.

4. Swarm formation with obstacle avoidance

In this section, a novel method for obstacle avoidance of unmanned vehicles is developed in three-dimensional space. Then by applying this approach, a problem of coordination formation control based on the behavioral structure for multiple unmanned vehicles with obstacle avoidance is studied.

4.1. Obstacle avoidance

We consider that there is an obstacle in unmanned vehicle's desired trajectory. The potential field with rotational vectors method is presented for obstacle avoidance of unmanned vehicles. The potential field method depends on repulsive force. When the repulsive force is in the opposite direction of approaching unmanned vehicle, the unmanned vehicle will stick in a local minimum position. To avoid this condition, the rotational vectors are presented to adjust the direction of the unmanned vehicle to avoid the obstacles. The rotational vectors around the obstacle adjust the direction of the unmanned vehicle to avoid the obstacle. Without loss of generality, we consider the obstacle as a rectangular solid in the direction of the x-, y- and z-axis of the Cartesian coordinate system. Its center and dimension can be detected and measured through the sensors of unmanned vehicles. As shown in Fig. 3, an ellipsoid is supposed which covers the vertices of obstacle with the minimum volume. The potential fields with rotational vectors are covered this ellipsoid and can be divided into two kinds of potential fields: the potential field which is parallel to x–y plane with rotational vectors and the potential field which is parallel to y–z plane with rotational vectors. Lemma 4.1 proposes the equation of ellipsoid with the minimum volume.

Lemma 4.1. *The equation of minimum volume ellipsoid that covers a rectangular solid is given as follows*:

$$\frac{1}{3v_1^2}(x-x_0)^2+\frac{1}{3v_2^2}\left(y-y_0\right)^2+\frac{1}{3v_3^2}(z-z_0)^2=1 \tag{14}$$

where (x_0, y_0, z_0) *is the center of the rectangular solid and* $(x_0 \pm v_1, y_0 \pm v_2, z_0 \pm v_3)$ *are its vertices.*

We consider an ellipsoid with implicit equation:

$$A^2(x-x_0)^2+B^2\left(y-y_0\right)^2+C^2(z-z_0)^2=1 \tag{15}$$

The volume of the ellipsoid is proportional to $1/ABC$. To get the minimum volume ellipsoid, $(ABC)^2$ should be the maximum. By inserting the coordinate of rectangular solid vertices, the

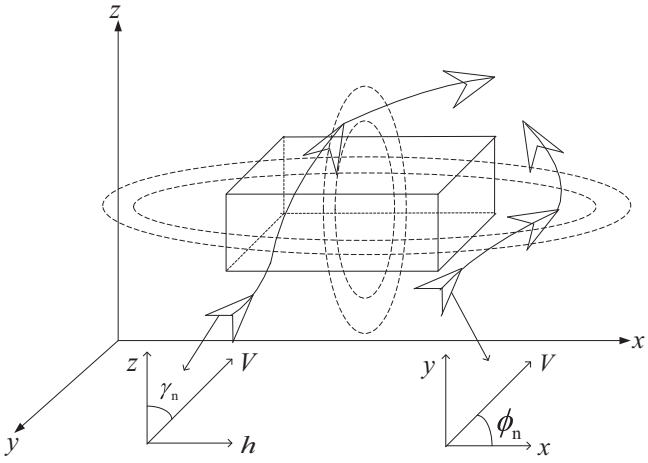

Fig. 3. The potential fields with rotational vectors around an obstacle.

equation can be induced as follows:

$$A^2v_1^2 + B^2v_2^2 + C^2v_3^2 = 1 \quad \Rightarrow \quad C^2 = \frac{1 - A^2v_1^2 - B^2v_2^2}{v_3^2} \tag{16}$$

The maximum $(ABC)^2$ can be gained by satisfying

$$\frac{\partial(ABC)^2}{\partial A} = 0, \quad \frac{\partial(ABC)^2}{\partial B} = 0 \tag{17}$$

Inserting Eq. (16) into Eq. (17), we deduce $A = \frac{1}{\sqrt{3v_1^2}}$, $B = \frac{1}{\sqrt{3v_2^2}}$. By substituting A^2 and B^2 to Eq. (16), we can obtain the desired result and prove Eq. (14).

Thus, we obtain the equation of ellipsoid covers the obstacle with minimum volume. It can be described as follows:

$$A^2(x - x_0)^2 + B^2(y - y_0)^2 + C^2(z - z_0)^2 = 1$$

where $A^2 = 1/3v_1^2$, $B^2 = 1/3v_2^2$, $C^2 = 1/3v_3^2$. The potential fields cover the obstacle are concentric to this ellipsoid and satisfying [17]

$$\tilde{A}^2(x - x_0)^2 + \tilde{B}^2(y - y_0)^2 + \tilde{C}^2(z - z_0)^2 = 1 \tag{18}$$

where $\frac{\tilde{A}}{\tilde{B}} = \frac{A}{B}$ and $\frac{\tilde{C}}{\sqrt{\tilde{A}^2 + \tilde{B}^2}} = \frac{C}{\sqrt{A^2 + B^2}}$. Hence, the potential fields with rotational vectors can be divided into the potential fields which are parallel to x–y plane with rotational vectors and potential fields which are parallel to y–z plane with rotational vectors. It is depicted in Fig. 3. In the potential fields which are parallel to x–y plane, the rotational vectors have two directions: clockwise direction and counterclockwise direction. The rotational vectors in clockwise direction can be stated as follows:

$$\begin{aligned} \dot{x} &= \frac{B}{A}(x - x_0) \\ \dot{y} &= -\frac{A}{B}(y - y_0) \\ \dot{z} &= 0 \end{aligned} \tag{19}$$

In the potential fields which are parallel to y–z plane, the rotational vectors have two directions: upward direction and downward direction. The rotational vectors in upward direction can be stated as follows:

$$\begin{aligned} \dot{x} &= \frac{C}{\sqrt{A^2 + B^2}}(z - z_0)\cos(\phi) \\ \dot{y} &= \frac{C}{\sqrt{A^2 + B^2}}(z - z_0)\sin(\phi) \\ \dot{z} &= -\frac{\sqrt{A^2 + B^2}}{C}(x - x_0)\cos(\phi) + \frac{\sqrt{A^2 + B^2}}{C}(y - y_0)\sin(\phi) \end{aligned} \tag{20}$$

To determine the direction of rotational vectors for the nth unmanned vehicle in the potential fields which are parallel to x–y plane, we use the direction angle ϕ_n to compare with the angle χ_n which between the tangent direction of the potential field and the horizon axis. $\phi_n = \arctan(\dot{y}_n, \dot{x}_n)$ and angle χ_n can be described as follows:

$$\chi_n = \arctan(y_0 - y_n,\ x_0 - x_n)$$

where χ_n and ϕ_n are shown in Fig. 4.

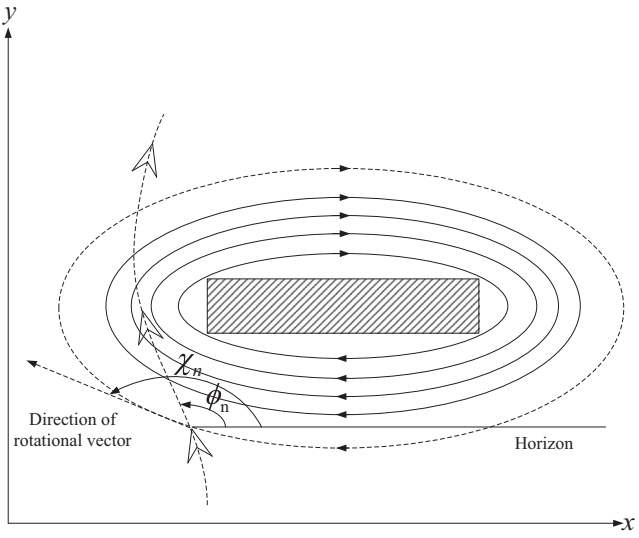

Fig. 4. The potential field which is parallel to the x–y plane with rotational vectors in clockwise direction around obstacle and trajectory of unmanned vehicle on x–y plane.

By comparing the angles χ_n and ϕ_n, the direction of the rotational vectors is reserved. Thus the clockwise or counterclockwise rotational vectors around the obstacles can be rewritten as follows:

$$\begin{aligned} f_{x_{nc}} &= \frac{\tilde{B}}{\tilde{A}}(y_n - y_0) = \frac{B}{A}(y_n - y_0) \\ f_{y_{nc}} &= -\frac{\tilde{A}}{\tilde{B}}(x_n - x_0) = -\frac{\tilde{A}}{\tilde{B}}(x_n - x_0), \quad |\phi_n - \chi_n| \le \frac{\pi}{2} \\ f_{z_{nc}} &= 0 \end{aligned} \tag{21}$$

and

$$\begin{aligned} f_{x_{ncc}} &= -\frac{\tilde{B}}{\tilde{A}}(y_n - y_0) = -\frac{B}{A}(y_n - y_0) \\ f_{y_{ncc}} &= \frac{\tilde{A}}{\tilde{B}}(x_n - x_0) = \frac{\tilde{A}}{\tilde{B}}(x_n - x_0) \quad \text{otherwise} \\ f_{z_{ncc}} &= 0 \end{aligned} \tag{22}$$

Similar to determining rotational vectors in clockwise or counterclockwise direction in the potential fields which are parallel to x–y plane, the rotational vectors in upward or downward direction of the nth unmanned vehicle are reserved by comparing direction angle ζ_n with the angle γ_n. γ_n is the angle between the tangent direction of the potential field and the horizon axis (Fig. 5):

$$\gamma_n = \arctan\left[\frac{C}{\sqrt{A^2+B^2}}(z_n - z_0), -\frac{\sqrt{A^2+B^2}}{C}(x_n - x_0)\cos(\phi) - \frac{\sqrt{A^2+B^2}}{C}(y_n - y_0)\sin(\phi)\right]$$

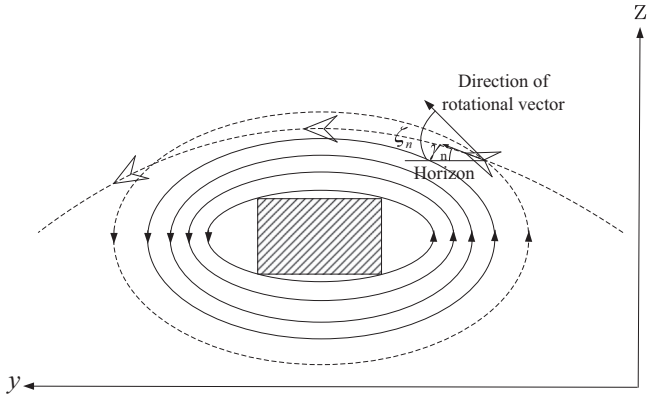

Fig. 5. Potential field which is parallel to y–z plane with rotational vectors in upward direction around obstacle and trajectory of unmanned vehicle, when $\dot{x}=0$.

The angle ζ_n can be described as

$$\zeta_n = \arctan\left(\frac{\dot{z}_n}{\sqrt{\dot{x}_n^2+\dot{y}_n^2}}\right)$$

The unmanned vehicles choose the direction of the rotational vectors in the potential field which is parallel to the y–z plane to avoid the obstacle by comparing the γ_n and ζ_n. The rotational vectors in upward direction or downward direction around the obstacles can be rewritten as follows:

$$\begin{aligned}
f_{x_{nt}} &= \frac{\tilde{C}}{\sqrt{\tilde{A}^2+\tilde{B}^2}}(z_n-z_0)\cos(\phi) = \frac{C}{\sqrt{A^2+B^2}}(z_n-z_0)\cos(\phi)\\
f_{y_{nt}} &= \frac{\tilde{C}}{\sqrt{\tilde{A}^2+\tilde{B}^2}}(z_n-z_0)\sin(\phi) = \frac{C}{\sqrt{A^2+B^2}}(z_n-z_0)\sin(\phi), \quad \left|\zeta_n-\gamma_n\right| \le \frac{\pi}{2}\\
f_{z_{nt}} &= -\frac{\sqrt{\tilde{A}^2+\tilde{B}^2}}{\tilde{C}}(x_n-x_0)\cos(\phi) - \frac{\sqrt{\tilde{A}^2+\tilde{B}^2}}{\tilde{C}}\left(y_n-y_0\right)\sin(\phi)\\
&= -\frac{\sqrt{A^2+B^2}}{C}(x_n-x_0)\cos(\phi) - \frac{\sqrt{A^2+B^2}}{C}\left(y_n-y_0\right)\sin(\phi)
\end{aligned} \tag{23}$$

and

$$\begin{aligned}
f_{x_{nb}} &= -\frac{\tilde{C}}{\sqrt{\tilde{A}^2+\tilde{B}^2}}(z_n-z_0)\cos(\phi) = -\frac{C}{\sqrt{A^2+B^2}}(z_n-z_0)\cos(\phi)\\
f_{y_{nb}} &= -\frac{\tilde{C}}{\sqrt{\tilde{A}^2+\tilde{B}^2}}(z_n-z_0)\sin(\phi) = -\frac{C}{\sqrt{A^2+B^2}}(z_n-z_0)\sin(\phi), \quad \text{otherwise}\\
f_{z_{nb}} &= \frac{\sqrt{\tilde{A}^2+\tilde{B}^2}}{\tilde{C}}(x_n-x_0)\cos(\phi) + \frac{\sqrt{\tilde{A}^2+\tilde{B}^2}}{\tilde{C}}\left(y_n-y_0\right)\sin(\phi)\\
&= \frac{\sqrt{A^2+B^2}}{C}(x_n-x_0)\cos(\phi) + \frac{\sqrt{A^2+B^2}}{C}\left(y_n-y_0\right)\sin(\phi)
\end{aligned} \tag{24}$$

Therefore, it is necessary for the unmanned aircraft to compare the two potential fields with rotational vectors, and choose a potential field which the smaller angle between its flight trajectory and the rotational vector at the unmanned aircraft position is acute, the rotational vectors can be stated as follows:

$$f_{nr} = f_{x_{nr}} i + f_{y_{nr}} j + f_{z_{nr}} k \tag{25}$$

Different trajectories can be generated by using different kinds of potential fields with rotational vectors in obstacle avoidance. The unmanned vehicle can avoid the obstacle by using the potential field which is parallel to x–y plane with rotational vectors in clockwise or counterclockwise direction:

$$f_{x_{nrxy}} = f_{x_{nc}}, \quad f_{y_{nrxy}} = f_{y_{nc}}, \quad f_{z_{nrxy}} = f_{z_{nc}}, \quad \phi_n \geq \chi_n$$
$$f_{x_{nrxy}} = f_{x_{ncc}}, \quad fy_{nrxy} = f_{y_{ncc}}, \quad f_{z_{nrxy}} = fz_{ncc}, \quad \phi_n < \chi_n$$

Or using the potential field which is parallel to the y–z plane with the rotational vectors in upward direction or in downward direction:

$$f_{x_{nryz}} = f_{x_{nt}}, \quad f_{y_{nryz}} = f_{y_{nt}}, \quad f_{z_{nryz}} = f_{z_{nt}}, \quad \zeta_n \geq \gamma_n$$
$$f_{x_{nryz}} = f_{x_{nb}}, \quad f_{y_{nryz}} = f_{y_{nb}}, \quad f_{z_{nryz}} = f_{z_{nb}}, \quad \zeta_n < \gamma_n$$

Every unmanned vehicle in formation has two obstacles avoidance trajectories. Following each obstacle avoidance trajectory, we compare the length from the entering point to the target point that exit the potential field:

$$f_{x_{nr}} = f_{x_{nrxy}}, \quad f_{y_{nr}} = f_{y_{nrxy}}, \quad f_{z_{nr}} = f_{z_{nrxy}}, \quad L_{yz} \geq L_{xy}$$
$$f_{x_{nr}} = f_{x_{nryz}}, \quad f_{y_{nr}} = f_{y_{nryz}}, \quad f_{z_{nr}} = f_{z_{nryz}}, \quad L_{yz} < L_{xy}$$

where L_{xy} is the length of obstacle avoidance trajectory by using the potential field which is parallel to x–y plane with rotational vectors, L_{yz} is the length of obstacle avoidance trajectory by using the potential field which is parallel to y–z plane with rotational vectors. Thus we modify and normalize the rotational vectors as follows:

$$f_n = f_{x_n} i + f_{y_n} j + f_{z_n} k = \frac{f_{x_{nr}}}{\|f_{nr}\|} i + \frac{f_{y_{nr}}}{\|f_{nr}\|} j + \frac{f_{z_{nr}}}{\|f_{nr}\|} k \tag{26}$$

We desire that the rotational vectors enlarge when unmanned vehicle is closer to the obstacle that require distance from unmanned vehicle to obstacle. It is denoted by r_n:

$$r_n = \sqrt{(x_n - x_0)^2} + (y_n - y_0)^2 + (z_n - z_0)^2$$

Therefore, the control force equations can be stated as follows: if $r_n \leq r_o$

$$f_{x_n}(oa) = f_{x_{ndesire}} + \frac{|f_{x_{ndesire}}| f_{x_n}}{r_n^2} \left(\frac{1}{r_n} - \frac{1}{r_0} \right)$$
$$f_{y_n}(oa) = f_{y_{ndesire}} + \frac{|f_{y_{ndesire}}| f_{y_n}}{r_n^2} \left(\frac{1}{r_n} - \frac{1}{r_0} \right)$$
$$f_{z_n}(oa) = f_{z_{ndesire}} + \frac{|f_{z_{ndesire}}| f_{z_n}}{r_n^2} \left(\frac{1}{r_n} - \frac{1}{r_0} \right)$$

else

$$\begin{aligned} f_{x_n}(oa) &= f_{x_{ndesire}} \\ f_{y_n}(oa) &= f_{y_{ndesire}} \\ f_{z_n}(oa) &= f_{z_{ndesire}} \end{aligned} \tag{27}$$

where r_0 is the range of ellipse potential field where the rotational vectors are effective. $f_{ndesire} = \left(f_{x_{ndesire}}, f_{y_{ndesire}}, f_{z_{ndesire}}\right)$ is the desired control force without obstacle avoidance. The term $\left(\frac{1}{r_n} - \frac{1}{r_0}\right)$ ensures the rotational vectors enlarge when unmanned vehicle is closer the obstacle.

Example 2. The initial position of an unmanned vehicle is (5, 4, 4), $M = 1, D = 1, k = 9$, the potential field range parameter $r_0 = 2$. The obstacle with $(20 \pm 3, 20 \pm 2, 5 \pm 1)$. The target position is denoted by p_t with $(x_t, y_t, z_t) = (20, 20, 5)$, we define the desired control force $f_{ndesire} = \left(f_{x_{ndesire}}, f_{y_{ndesire}}, f_{z_{ndesire}}\right)$ as follows:

$$\begin{aligned} f_{x_{ndesire}} &= \frac{x_t - x_n}{\sqrt{(x_n - x_t)^2 + (y_n - y_t)^2 + (z_n - z_t)^2}} \\ f_{y_{ndesire}} &= \frac{y_t - y_n}{\sqrt{(x_n - x_t)^2 + (y_n - y_t)^2 + (z_n - z_t)^2}} \\ f_{z_{ndesire}} &= \frac{z_t - z_n}{\sqrt{(x_n - x_t)^2 + (y_n - y_t)^2 + (z_n - z_t)^2}} \end{aligned} \tag{28}$$

Fig. 6 shows the unmanned vehicle avoids the obstacle and settles the target position by using the proposed method. Two kinds of potential fields with rotational vectors are effective. The length of trajectory that unmanned vehicle using the potential field which is parallel to x–y plane with rotational vectors in clockwise direction is 25.92 and the length of trajectory that unmanned vehicle using the potential field which is parallel to y–z plane with rotational vectors in upward direction is 22.55. We will choose the shorter trajectory among them.

It is noted that if the ellipse potential field can cover the obstacle with any shape, the proposed method of obstacle avoidance is effective.

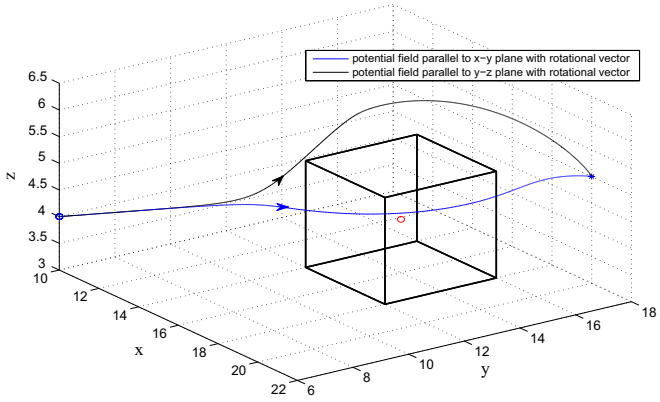

Fig. 6. Trajectories of obstacle avoidance by using two kinds of potential fields with rotational vectors.

4.2. Behavioral structure

Based on the proposed method, we want unmanned vehicles to reconfigure the formation after passing the potential field with rotational vectors. The control force can be adjusted smoothly when it shifts from obstacle avoidance to formation reconfiguration.

To solve this problem, we select the target position from virtual leader's trajectory during the process of avoiding obstacle. To avoid the collision among unmanned vehicles, the target should be out of the potential field with rotational vectors. Therefore, the strategy of unmanned vehicles in behavioral structures can be stated as follows: if $r_{\min} \le r_o$ ($r_{\min} =$ minimum of r_n, $n \in \{1, 2, \ldots, N\}$)

$$\begin{aligned} f_{x_n} &= f_{x_n}(oa) \\ f_{y_n} &= f_{y_n}(oa) \\ f_{z_n} &= f_{z_n}(oa) \end{aligned}$$

else (after passing the obstacle)

$$\begin{aligned} x_n &= f_{x_n}(vs) \\ f_{y_n} &= f_{y_n}(vs) \\ f_{z_n} &= f_{z_n}(vs) \end{aligned} \tag{29}$$

In the process of obstacle avoidance, the virtual leader's position can be stated as follows:

$$x_v = \frac{1}{N}\sum_{n=1}^{N} x_n, \quad y_v = \frac{1}{N}\sum_{n=1}^{N} y_n, \quad z_v = \frac{1}{N}\sum_{n=1}^{N} z_n \tag{30}$$

5. Simulation result

This section shows the performance of the proposed approaches in different scenarios.

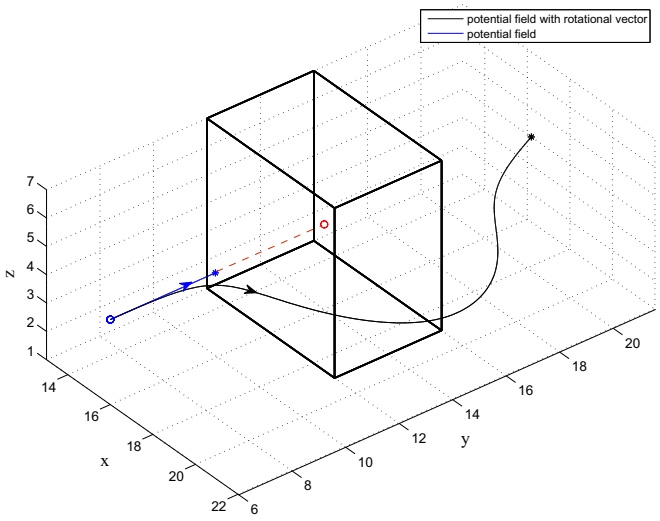

Fig. 7. Unmanned vehicle avoids the obstacle without the influence of local minimum position.

Scenario 1: Consider an unmanned vehicle with initial position (16,6,4). The position of obstacle center is (16,14,4). The input control force is (0,2,0). The unmanned vehicle move toward the center of the obstacle. If traditional potential field is implied, it cancels the input force. The unmanned vehicle will stay in a local minimum position. Fig. 7 confirms unmanned vehicle avoids the obstacle without the influence of local minimum position by using the potential field which is parallel to x–y plane with rotational vectors in counterclockwise direction.

Scenario 2: We show that the swarming of the unmanned vehicles can transform into a new formation structure when an unmanned vehicle enters the formation. Consider the four unmanned vehicles with initial positions (2,2,2), (0,2,3), (1,2,5), (2,3,2). The dynamical

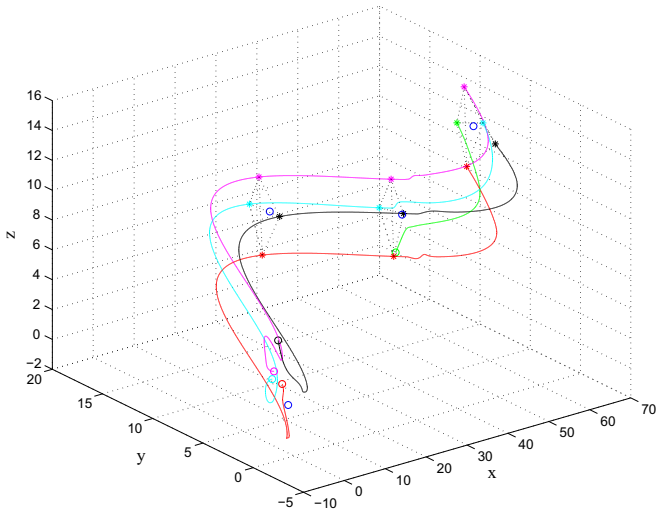

Fig. 8. Unmanned vehicle formation flying in Scenario 2.

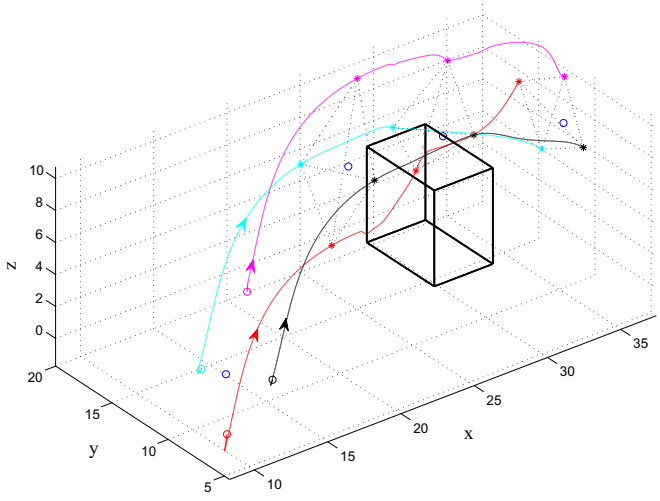

Fig. 9. Formation flying with obstacle avoidance by using the potential field method in Scenario 3.

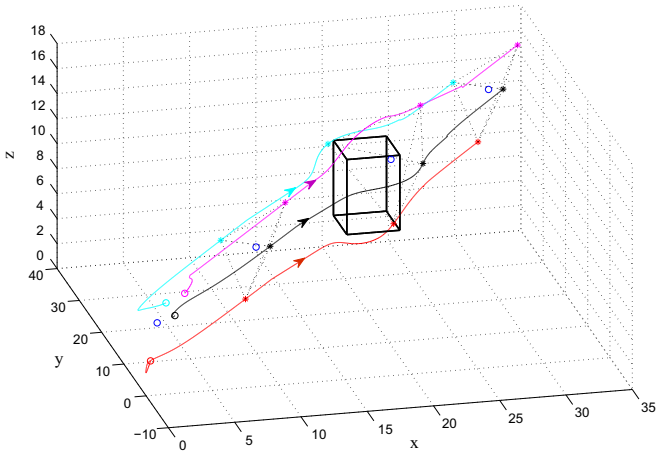

Fig. 10. Formation flying with obstacle avoidance and formation reconfiguration by using the potential field with rotational vectors in Scenario 3.

equations and input control force are given in Eq. (28). The initial position of virtual leader is (1,1,1). According to Eq. (13), $f_{x_v} = 10, f_{y_v} = 10 * \sin\left(1/8x_v\right), f_{z_v} = 2$. Without loss the generality, we set $M = 1, D = 1, k_r = 5, k_s = 5, k = 9$. Fig. 8 shows that four unmanned vehicles build up a formation and move as a regular tetrahedron. An unmanned vehicle enters in the formation arbitrarily at some point. The distances between the unmanned vehicles are regulated autonomously to reach a triangular bipyramid formation. This implies that unmanned vehicles can join or exit the formation without specific identities.

Scenario 3: Consider an obstacle with vertices $(x_c \pm 2, y_c \pm 3, z_c \pm 3)$. Fig. 9 is real-time trajectories of formation by using the potential field method. Fig. 10 is the real-time trajectories of formation by using the proposed method in this paper. The formation can easily switch to an obstacle avoidance strategy when formation is close to the obstacle (as illustrated in Fig. 10). Every unmanned vehicle has a smooth and optimal trajectory without locating in local minimum position. In comparison to Fig. 9, the velocity commands are smooth and reasonable by using the proposed method.

6. Conclusion

We have considered the problem of unmanned vehicles formation control based on behavioral and virtual structure in three-dimensional space. A control method for formation of unmanned vehicles was presented that the attractive forces led unmanned vehicles toward a spherical surface and the repulsive force kept safe distance between identical electric charges. By using the proposed method, unmanned vehicles arrived at the balance points which are evenly distributed on the spherical surface. Simulation results showed that the unmanned vehicles built up and maintained the formation without requiring specific orders or desired positions of unmanned vehicles by using the proposed method. Compared to similar techniques, although obstacles avoidance approaches used potential fields, the proposed approach prevented the collision with the obstacles and led the unmanned vehicles to move toward their desired targets in smoother and shorter trajectories without sticking in local minimum positions. Future work will include extensions to formation of UAVs, AUVs and satellites with obstacle avoidance.

Acknowledgements

The authors would like to thank the referees for their valuable and helpful comments, which have improved the presentation of this paper. The work was supported by the National Basic Research Program of China (973 Program) (2012CB720000), the National Natural Science Foundation of China (61225015 and 61105092), and Foundation for Innovative Research Groups of the National Natural Science Foundation of China (Grant No. 61321002).

References

[1] E.J. Forsmo, E.I. Grotli, T.I. Fossen, T.A. Johansen, Optimal search mission with unmanned aerial vehicles using mixed integer linear programming, in: International Conference on Unmanned Aircraft Systems (ICUAS), 2013, pp. 253–259.
[2] Z. Peng, G. Wen, A. Rahmani, Y. Yu, Leader–follower formation control of nonholonomic mobile robots based on a bioinspired neurodynamic based approach, Robot. Autonom. Syst. 61 (9) (2013) 988–996.
[3] X. Bian, C. Mou, Z. Yan, H. Wang, Formation coordinated control for multi-AUV based on spatial curve path tracking, OCEANS 2011 (2011) 1–6.
[4] S. Monteiro, E. Bicho, A dynamical systems approach to behavior-based formation control, in: IEEE International Conference on Robotics and Automation, vol. 3, 2002, pp. 2606–2611.
[5] O. Cetin, I. Zagli, G. Yilmaz, Establishing obstacle and collision free communication relay for UAVs with artificial potential fields, J. Intell. Robot. Syst. 69 (1–4) (2013) 361–372.
[6] C.C. Cheah, S.P. Hou, J.J.E. Slotine, Region-based shape control for a swarm of robots, Automatica 45 (10) (2009) 2406–2411.
[7] H. Rezaee, F. Abdollahi, A decentralized cooperative control scheme with obstacle avoidance for a team of mobile robots, IEEE Trans. Ind. Electron. 61 (1) (2014) 347–354.
[8] J. Hu, G. Feng, Distributed tracking control of leader–follower multi-agent systems under noisy measurement, Automatica 46 (8) (2010) 1382–1387.
[9] R. Cui, Ge.S. Sam, Ee. Voon, B How, Leader–follower formation control of underactuated autonomous underwater vehicles, Ocean Eng. 37 (17) (2010) 1491–1502.
[10] H. Rezaee, F. Abdollahi, Mobile robots cooperative control and obstacle avoidance using potential field, in: International Conference on Advanced Intelligent Mechatronics (AIM), 2011, pp. 61–66.
[11] F. Flacco, T. Kroger, A. De Luca, O. Khatib, A depth space approach to human–robot collision avoidance, in: International Conference on Robotics and Automation (ICRA), 2012, pp. 338–345.
[12] M.S. Couceiro, R.P. Rocha, N.M. Ferreira, A novel multi-robot exploration approach based on particle swarm optimization algorithms, in: International Symposium on Safety, Security, and Rescue Robotics (SSRR), 2011, pp. 327–332.
[13] A. Widyotriatmo, K.-S. Hong, Navigation function-based control of multiple wheeled vehicles, IEEE Trans. Ind. Electron. 58 (5) (2011) 1896–1906.
[14] J. Ghommam, H. Mehrjerdi, M. Saad, F. Mnif, Formation path following control of unicycle-type mobile robots, Robot. Autonom. Syst. 58 (5) (2010) 727–736.
[15] H. Mehrjerdi, J. Ghommam, M. Saad, Nonlinear coordination control for a group of mobile robots using a virtual structure, Mechatronics 21 (7) (2011) 1147–1155.
[16] D.V. Dimarogonas, Sufficient conditions for decentralized potential functions based controllers using canonical vector fields, IEEE Trans. Autom. Control 57 (10) (2012) 2621–2626.
[17] H. Rezaee, F. Abdollahi, Adaptive artificial potential field approach for obstacle avoidance of unmanned aircrafts, in: International Conference on Advanced Intelligent Mechatronics (AIM), 2012, pp. 1–6.
[18] E.J. Gomez, F.M. Santa, F.H.M. Sarmiento, A comparative study of geometric path planning methods for a mobile robot: potential field and Voronoi diagrams, in: International Congress of Engineering Mechatronics and Automation (CIIMA), 2013, pp. 1–6.